

A nuclear magnetic resonance investigation of hydrogen diffusion in the A15 compound Ti_3Ir

This article has been downloaded from IOPscience. Please scroll down to see the full text article.

1992 J. Phys.: Condens. Matter 4 6919

(<http://iopscience.iop.org/0953-8984/4/33/006>)

View [the table of contents for this issue](#), or go to the [journal homepage](#) for more

Download details:

IP Address: 171.66.16.96

The article was downloaded on 11/05/2010 at 00:24

Please note that [terms and conditions apply](#).

A nuclear magnetic resonance investigation of hydrogen diffusion in the A15 compound Ti_3Ir

D Guthardt, D Beisenherz and H Wipf

Institut für Festkörperphysik, Technische Hochschule Darmstadt, Hochschulstraße 6, W-6100 Darmstadt, Federal Republic of Germany

Received 24 March 1992

Abstract. The spin–lattice relaxation time of hydrogen in Ti_3IrH_x was determined from pulsed nuclear magnetic resonance measurements carried out between 5 and 630 K ($x = 0.55, 3.0$ and 3.5 ; $5 \text{ K} < T < 630 \text{ K}$). The measured relaxation rates can be described by a superposition of Korringa relaxation and dipolar relaxation due to hydrogen diffusion. The Korringa relaxation times $T_{1,c}$ obey the relation $T_{1,c}T = 87 \pm 4 \text{ s K}$, $124 \pm 8 \text{ s K}$ and $145 \pm 8 \text{ s K}$ for $x = 0.55, 3.0$ and 3.5 , respectively. The dipolar relaxation rates were analysed with the help of a modified BPP model, yielding the mean residence times of the hydrogen between about 200 and about 500 K. The mean residence times depend on the hydrogen concentration x . They can be described by an Arrhenius relation with activation energies of $155 \pm 15 \text{ meV}$ (for $x = 0.55$), $365 \pm 30 \text{ meV}$ ($x = 3.0$) and $265 \pm 25 \text{ meV}$ ($x = 3.5$).

1. Introduction

This paper reports the results of a study investigating hydrogen diffusion in the A15 compound Ti_3Ir . The study was carried out with the help of pulsed nuclear magnetic resonance (NMR) measurements of the spin–lattice relaxation time T_1 of the hydrogen nuclei. Compounds with the cubic A15 structure, such as Nb_3Sn or V_3Ga , represent an important class of materials comprising, in particular, technologically interesting superconductors (see [1] for a review article). In fact, Ti_3Ir is also a superconductor with a transition temperature of about 4 K [1].

The solubility of hydrogen in Ti_3Ir and the structure of the hydrogenated compounds Ti_3IrH_x were recently investigated up to hydrogen concentrations $x = 3.9$ (x is the H-to- Ti_3Ir ratio) [2, 3]. It was found that the absorbed hydrogen did not change the cubic A15 structure of the host metal and that the lattice parameter increases linearly with increasing x . Similar findings have been reported from other A15 hydride systems [2, 4–9]. The measurements on Ti_3Ir demonstrated further a room-temperature miscibility gap in the range $0.9 < x < 2.3$. The results of the present study suggest that the concentration range of the miscibility gap increases with falling temperature.

Neutron diffraction measurements on the A15 hydride Nb_3SnH_x revealed that the hydrogen occupies tetrahedral sites surrounded by four (nearest-neighbour) Nb atoms [6]. For the isostructural compound Ti_3Ir , at present investigated, this type of interstitial site is shown in figure 1. Since there are three such sites per Ti_3Ir formula unit, the maximum hydrogen concentration expected for sole occupation of these

sites is $x = 3$. This limit shows that the hydrogen in Ti_3Ir cannot exclusively occupy tetrahedral interstitial sites such as those indicated in figure 1 since the hydrogen concentrations investigated in [2, 3] ranged up to $x = 3.9$ (without any changes in the A15 structure of the Ti_3Ir host compound). The system Ti_3IrH_x differs in this respect from the other A15 hydrides for which concentrations above $x = 3$ have not been reported so far. This peculiar behaviour of Ti_3IrH_x was one of the chief reasons for the present study.

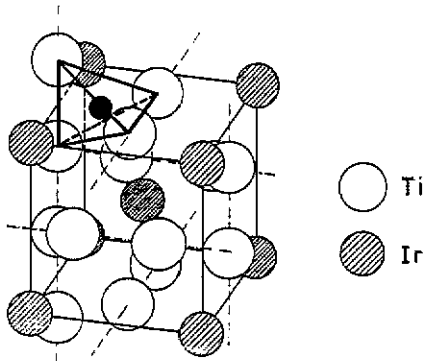


Figure 1. Cubic unit cell of the A15 compound Ti_3Ir . The small full circle indicates the position of a tetrahedral interstitial site.

The diffusion of hydrogen in A15 compounds was investigated in two previous studies [10, 11]. From the time dependence of hydrogen (and deuterium) absorption measurements, the diffusion coefficient of hydrogen (deuterium) in Ti_3Ir was determined in the temperature range between 670 and 1170 K [10]. The measurements, carried out with low hydrogen concentrations (up to $x = 0.02$), demonstrated that the diffusion coefficient of the hydrogen can be described by an Arrhenius relation $D = D_0 \exp(E/k_B T)$ with $D_0 = 2.2 \pm 0.4 \text{ cm}^2 \text{ s}^{-1}$ and $E = 0.25 \pm 0.02 \text{ eV}$. In the case of the A15 compound Nb_3Sn , the dynamics of the interstitial hydrogen were studied by internal-friction measurements [11]. The study was performed with frequencies between about 50 and about 4000 Hz, and it revealed a hydrogen-related internal-friction peak in the temperature range around 260 K.

2. Sample preparation and experimental details

The measurements were carried out on three different Ti_3IrH_x samples with $x = 0.55 \pm 0.05$, 3.0 ± 0.1 and 3.5 ± 0.1 . The Ti_3Ir host compound was prepared from titanium with a nominal purity of 99.98% according to the manufacturer (MRC) and from iridium with a nominal purity of 99.9% (Heraeus). The two constituents were, in their stoichiometric weight ratio, repeatedly melted (at least 20 times) in a water-cooled copper crucible located in an induction furnace (argon atmosphere of about 1 bar). The alloys were rotated between the individual melting processes to improve homogenization. For further homogenization, the alloys were subsequently annealed for about 30 min first at about 1400 °C and then at about 1300 °C [12]. Thereafter, they were slowly cooled to room temperature.

For hydrogen doping, the prepared Ti_3Ir material was first pulverized and then exposed to hydrogen gas in a vacuum system at elevated temperatures. For each of

the three desired concentrations x , the hydrogen gas pressure and the temperature were adjusted according to the solubility isotherms in [2]. The precise values of x were determined after the doping procedure by vacuum extraction of small fractions of the prepared Ti_3IrH_x powder. X-ray diffraction measurements, carried out at room temperature, demonstrated in all cases the A15 structure of the material.

The NMR measurements were performed in the range from 5 to 630 K with a standard Bruker pulse spectrometer at frequencies of 11.899 and 54.795 MHz. The spin-lattice relaxation time T_1 of the protons was determined by a $180^\circ-90^\circ$ pulse method. The Ti_3IrH_x samples investigated were encapsulated in quartz glass containers which were positioned in a single coil for both pulse generation and signal pick-up. Table 1 presents a compilation of the investigated samples and the applied frequencies, together with experimental results to be discussed later.

Table 1. Compilation of data for the samples investigated, showing the resonance frequencies f studied, the constant $C^{-1} = TT_{1,e}$ describing the Korringa relaxation according to equation (2), and the activation energy E and the pre-exponential factor τ_0 of the mean residence time $\tau = \tau_0 \exp(E/k_B T)$.

Sample	f (MHz)	$TT_{1,e}$ (s K)	E (eV)	τ_0 (s)
$Ti_3IrH_{0.55}$	54.795	87 ± 3	0.155 ± 0.015	$\approx 4.4 \times 10^{11}$
$Ti_3IrH_{3.0}$	11.889	124 ± 6	0.356 ± 0.025	$\approx 1.7 \times 10^{13}$
$Ti_3IrH_{3.0}$	54.795		0.375 ± 0.030	$\approx 4.8 \times 10^{13}$
$Ti_3IrH_{3.5}$	54.795	145 ± 6	0.265 ± 0.020	$\approx 1.2 \times 10^{12}$

3. Theoretical background

In the present experimental situation, the proton relaxation rate T_1^{-1} can be decomposed into two terms:

$$T_1^{-1} = T_{1,e}^{-1} + T_{1,d}^{-1} \quad (1)$$

where $T_{1,e}^{-1}$ describes the Korringa relaxation with the conduction electrons and $T_{1,d}^{-1}$ results from a dipolar interaction between the diffusing protons and a dipolar interaction between the protons and the nuclei of the host compound. The Korringa relaxation rate is proportional to the temperature T according to [13]:

$$T_{1,e}^{-1} = CT. \quad (2)$$

This temperature dependence allows experimental separation of the two relaxation rates in equation (1). The dipolar relaxation rate is given by [13-18]

$$T_{1,d}^{-1} = \hbar^2 \gamma_H^4 I_H (I_H + 1) \left[\frac{3}{2} J_{HH}^{(1)}(\omega_H) + \frac{3}{2} J_{HH}^{(2)}(2\omega_H) \right] + \hbar^2 \gamma_H^2 \sum_i \gamma_{M_i}^2 I_{M_i} (I_{M_i} + 1) \times \left[\frac{1}{12} J_{HM_i}^{(0)}(\omega_H - \omega_{M_i}) + \frac{3}{2} J_{HM_i}^{(1)}(\omega_H) + \frac{3}{4} J_{HM_i}^{(2)}(\omega_H + \omega_{M_i}) \right] \quad (3)$$

where $J_{HH}^{(j)}(\omega)$ and $J_{HM_i}^{(j)}(\omega)$ are the Fourier transforms of the correlation functions of the fluctuating local magnetic dipolar fields associated with the interaction between

the protons (subscript H) or between the protons and the various host compound nuclei of type i (subscript M_i). γ_H and γ_{M_i} are the gyromagnetic ratios of the protons and the respective host compound nuclei, I_H and I_{M_i} are the corresponding spin quantum numbers, and $\omega_H = \gamma_H B$ and $\omega_{M_i} = \gamma_{M_i} B$ are the corresponding spin precession frequencies in the applied magnetic field B .

Within a modified Bloembergen-Purcell-Pound (BPP) model, the dipolar relaxation rate $T_{1,d}^{-1}$ in equation (3) can be written as a function of the mean residence time τ of the hydrogen according to [15, 17]

$$T_{1,d}^{-1} = (\gamma_H^2/\omega_H)[\frac{3}{2}M_{HH}f_H(\omega_H\tau) + M_{HM}f_M(\omega_H\tau)]. \quad (4)$$

The quantities $f_H(\omega_H\tau)$ and $f_M(\omega_H\tau)$ are

$$f_H(\omega_H\tau) = 2\omega_H\tau/[4 + (\omega_H\tau)^2] + 2\omega_H\tau/[1 + (\omega_H\tau)^2] \quad (5a)$$

$$f_M(\omega_H\tau) = (\omega_H\tau/2)/[1 + (1 - \gamma_M/\gamma_H)^2(\omega_H\tau)^2] + (3\omega_H\tau/2)/[1 + (\omega_H\tau)^2] \\ + 3\omega_H\tau/[1 + (1 + \gamma_M/\gamma_H)^2(\omega_H\tau)^2] \quad (5b)$$

whereas M_{HH} and M_{HM} are lattice sums given by

$$M_{HH} = \frac{3}{5}\hbar^2\gamma_H^2I_H(I_H + 1)p_H \sum_j r_j^{-6} \quad (6a)$$

$$M_{HM} = \frac{4}{15}\hbar^2 \sum_i \gamma_{M_i}^2I_{M_i}(I_{M_i} + 1)p_{M_i} \sum_j r_j^{-6}. \quad (6b)$$

The summation over j in equations (6a) and (6b) extends over all the distances r_j between a given proton and the sites that can be occupied by other protons (equation (6a)) or by the host compound nuclei (equation (6b)), and the quantities p_H and p_{M_i} are the probabilities that these sites are actually occupied by a proton or by a host compound nucleus of type i , respectively (note that i differentiates also between different isotopes).

The modified BPP model leading to equations (4)–(6) is common for the analysis of the spin-lattice relaxation rate $T_{1,d}^{-1}$ of diffusing interstitial atoms [14–18]. The model assumes a random distribution of the hydrogen interstitials, spatial isotropy and an exponential decay of the correlation functions of the fluctuating local magnetic dipolar fields. The two other most important assumptions are that the correlation time of these correlation functions is half the mean residence time τ of the hydrogen in the case of the dipolar proton-proton interactions, and identical with τ for the interaction between the protons and the nuclei of the host compound [16]. These different assumptions reflect the fact that the correlation in the case of the proton-proton interaction decays more rapidly since both of the interacting particles are diffusing. The fact that the correlation time in the case of the proton-proton interaction is assumed to be $\tau/2$ is also the reason why the present expression for $f_H(\omega_H\tau)$ differs from the corresponding expression in [15, 17].

4. Experimental results and discussion

Figure 2 shows the results for the spin-lattice relaxation rate T_1^{-1} of the Ti_3IrH_x sample with $x = 3.0$ in a plot versus temperature. The data for this sample were

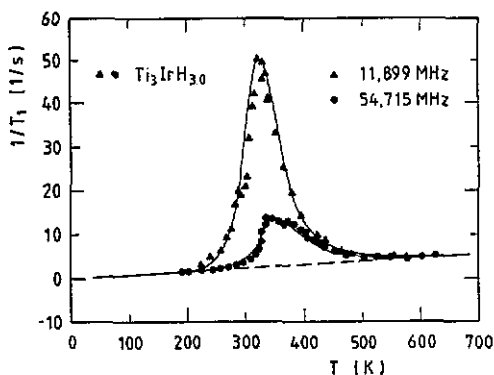


Figure 2. Spin-lattice relaxation rates T_1^{-1} of the Ti_3IrH_x sample with $x = 3.0$ in a plot versus temperature, where the data were taken at frequencies of 11,899 and 54,795 MHz: —, fitted curves for T_1^{-1} considering both Korringa relaxation and nuclear dipolar relaxation; - - -, frequency-independent contribution from Korringa relaxation.

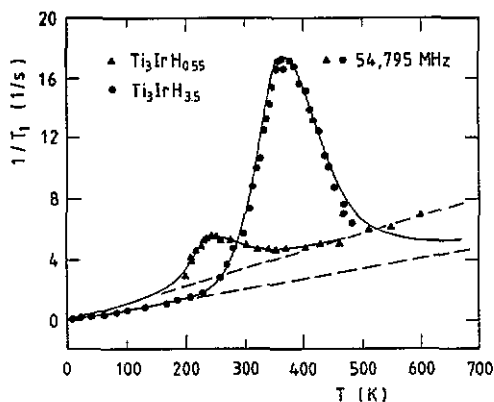


Figure 3. Spin-lattice relaxation rates T_1^{-1} of the Ti_3IrH_x samples with $x = 0.55$ and 3.5 in a plot versus temperature, where the data were taken at a frequency of 54,795 MHz: —, fitted curves for T_1^{-1} considering both Korringa relaxation and nuclear dipolar relaxation; - - -, contributions from Korringa relaxation.

collected at both of the investigated frequencies, 11,899 and 54,795 MHz. The results of the measurements on the two other samples ($x = 0.55$ and 3.5), carried out only at 54,795 MHz, are presented in figure 3.

The spin-lattice relaxation rates T_1^{-1} of the sample with the highest concentration $x = 3.5$ could be measured down to the lowest investigated temperature of about 5 K. In the case of the other two concentrations ($x = 0.55$ and 3.0), on the other hand, it was found that the decay of longitudinal magnetization had to be described by two different relaxation rates below about 200 K. Such a behaviour is expected in the presence of a miscibility gap where the sample decomposes into two phases with different hydrogen concentrations. The results suggest therefore that the concentration range of the miscibility gap ($0.9 < x < 2.3$ at room temperature [2, 3]) widens with decreasing temperature, so that the samples with $x = 0.55$ and 3.0 were actually in the miscibility gap below about 200 K. As a consequence of this behaviour, figures 2 and 3 do not show results for these two samples at temperatures below about 200 K where it was not possible to describe the decay of the longitudinal relaxation with a single spin-lattice relaxation rate T_1^{-1} .

For the sample with the highest concentration $x = 3.5$, the equilibrium hydrogen gas pressure rises steeply with increasing temperature (the pressure has already exceeded 1 bar at about 370 K [2]). For this reason, measurements on this sample were not performed above about 490 K in order to avoid explosion of the quartz glass container.

For the quantitative analysis of the spin-lattice relaxation rates T_1^{-1} in figures 2 and 3, we performed first a separation between the Korringa relaxation rate $T_{1,e}^{-1} = CT$, which is linear in temperature T , and the dipolar relaxation rate $T_{1,d}^{-1}$. The separation was based on the fact that the dipolar relaxation rate $T_{1,d}^{-1}$ is expected to be responsible for the respective relaxation maxima in figures 2 and 3, and that $T_{1,d}^{-1}$ becomes negligible far below and above these maxima. The contributions that

we find for the Korringa relaxation rate $T_{1,e}^{-1} = CT$ according to this criterion are indicated by the broken lines in figures 2 and 3. The values of the constants $C^{-1} = TT_{1,e}$ for the individual samples are also listed in table 1. For the sample with $x = 3.0$, the contribution from the Korringa relaxation could be derived from data for the total relaxation rate T_1^{-1} measured on both sides of the relaxation maxima (see figure 2). As required, the Korringa relaxation rate is also identical for both investigated frequencies. In the case of the samples with $x = 0.55$ and 3.5 (figure 3), the Korringa relaxation rate could be determined only from T_1^{-1} data either above or below the respective relaxation maximum. However, the quality of the data did allow a reliable determination of the Korringa relaxation rate also in these less favourable cases.

According to the above discussion, the differences between the total spin-lattice relaxation rate T_1^{-1} and the Korringa relaxation rate $T_{1,e}^{-1}$ for the data in figures 2 and 3 must be attributed to the dipolar relaxation rate $T_{1,d}^{-1}$. For a given mean residence time τ , the latter quantity can be calculated with the modified BPP model of section 3. The model requires, in principle, knowledge of the interstitial sites of the hydrogen. The fact that these sites are actually not known in the case of the present system Ti_3IrH_x means that we had to rely on plausible assumptions. Before explaining the assumptions that we made, we point out that the numerical results obtained for $T_{1,d}^{-1}$ are quite insensitive with respect to the specific type of interstitial site [14–18]. This means that the values of the mean residence time τ , which follow from our subsequent analysis, can essentially be considered to be correct even though they do actually imply invalid assumptions on the interstitial sites of the hydrogen.

We calculated the dipolar relaxation rate $T_{1,d}^{-1}$ under the assumption that the hydrogen is located on tetrahedral sites such as those shown in figure 1. The assumption cannot be entirely correct according to our discussion in section 1. However, it was made since we do not have any experimental indication which interstitial—or additional interstitial—sites are occupied by the hydrogen in the case of the present system Ti_3IrH_x . The above assumption means that the summation in equation (6a) extends over the distances r_j from one tetrahedral site to all the other sites, and that the value of the occupation probability p_H is $x/3$. In the case of the sample with $x = 3.5$, this leads to an unphysical occupation probability $p_H > 1$ which, however, is irrelevant in the light of the previous discussion. The calculation of the dipolar relaxation rate requires further, according to equation (6b), a summation over the distances r_j between a tetrahedral interstitial site and the lattice sites of the Ti_3Ir host compound, with consideration first of the actual Ti and Ir positions and second of the natural abundances and nuclear parameters of the isotopes of the two respective elements. We note also that the numerical calculations are extremely simplified by the fact that the high (negative) power of the distances r_j causes a rapid convergence of the (infinite) summation.

The above assumptions establish a definite relationship between the dipolar relaxation rate $T_{1,d}^{-1}$ and the mean residence time τ , which serves as the basis for the analysis of the data in figures 2 and 3. However, it is important to point out that the absolute values of the calculated relaxation rate $T_{1,d}^{-1}$ are not really reliable. This is exemplified by a comparison between the maxima of the calculated dipolar relaxation rates (equations (4)–(6)) with the corresponding maxima derived from the experimental data in figure 2 or 3. The comparison shows that the calculated maxima deviate in fact by up to 20% from the experimental maxima (the calculated maximum exceeds the experimental maximum for the $Ti_3IrH_{0.55}$ and $Ti_3IrH_{3.0}$ samples, and it

is smaller than the experimental maximum in the case of the $Ti_3IrH_{3.5}$ sample). Such discrepancies are quite common for calculated dipolar relaxation rates [14–18], and they may, in the present situation, result from general deficiencies in the assumptions underlying the modified BPP model or, more specifically, from the fact that our calculation did account for the (average) hydrogen-induced lattice expansion [2, 3] but not for any local strains closely around a hydrogen interstitial. As a consequence of these considerations, we assumed that the theoretical dipolar relaxation rates for each sample, and frequency, can be multiplied by a constant to be considered as a fitting parameter.

The actual derivation of the mean residence time τ from our data was carried out under the assumption of an Arrhenius relationship $\tau = \tau_0 \exp(E/k_B T)$ for the mean residence time. The values of E and τ_0 were then obtained from a fit to the data in figures 2 and 3. The full curves in these figures show the resulting fitted curves, and the numerical fitted results for E and τ_0 are presented in table 1. We point out that the fitted results for the sample with $x = 3.0$, which were obtained with two different frequencies, agree within experimental accuracy. Figure 4 shows an Arrhenius plot of the inverse mean residence times τ^{-1} that were derived for the three investigated samples (full lines). The inverse mean residence times are indicated only in the temperature ranges in which they could meaningfully be determined from the dipolar relaxation rates. The figure shows finally again the reasonable agreement between the inverse mean residence times determined at two different frequencies for the sample with $x = 3.0$.

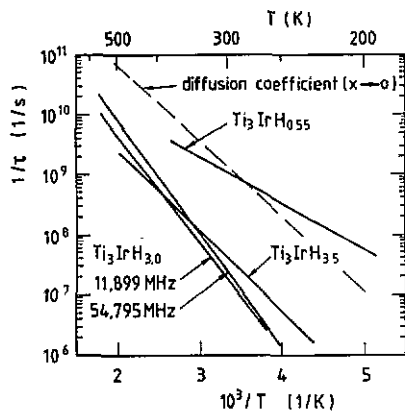


Figure 4. Arrhenius plot of inverse mean residence time τ^{-1} : —, results for the three present samples (in the case of the sample with $x = 3.0$, τ^{-1} could independently be derived from measurements with two different frequencies; the results for τ^{-1} are indicated only in those temperature ranges in which they could meaningfully be determined from the dipolar relaxation rates); - - -, extrapolated values of τ^{-1} , calculated according to equation (7) from data for the diffusion coefficient of the hydrogen ($x \leq 0.02$; $670 \text{ K} \leq T \leq 1170 \text{ K}$) [10].

The present values of τ^{-1} can be compared with previous results for the diffusion coefficient D of hydrogen in Ti_3Ir , measured in the temperature range between 670 and 1170 K at low hydrogen concentrations ($x \leq 0.02$; $E = 0.25 \pm 0.02 \text{ eV}$) [10]. Since we do not know the actual interstitial sites of the hydrogen, we relate the diffusion coefficient D to the inverse mean residence time τ^{-1} according to

$$\tau^{-1} = 6D/d^2 \quad (7)$$

where we assume that d is given by the shortest distance between tetrahedral sites such as those indicated in figure 1 ($d = a/2 \simeq 2.5 \text{ \AA}$, where a is the lattice parameter). The above relation can be expected to be sufficiently valid for the purpose of the

present discussion. The broken line in figure 4 shows extrapolated values of τ^{-1} which are calculated according to equation (7) from the (high-temperature) results for the diffusion coefficient [10]. The comparison of the data in figure 4 exhibits a distinct concentration dependence. It is particularly found that τ^{-1} is higher at low hydrogen concentrations, at least in the temperature range of the present measurements.

We consider finally the internal-friction study on the related A15 hydride system Nb_3SnH_x [11]. The study demonstrated a hydrogen-induced internal-friction peak in the temperature range around 260 K, observed for frequencies between about 50 and about 4000 Hz. If this peak is due to a type of Snoek relaxation, the inverse mean residence time τ^{-1} at the peak temperature should essentially be given by the angular frequency of the measurement, i.e. τ^{-1} should be in the range between 3×10^2 and $3 \times 10^4 \text{ s}^{-1}$. The comparison with figure 4 shows that these values for τ^{-1} are, at the same temperature, at least two orders of magnitude smaller than those of the present study. This may reflect the fact that the hydrogen in the compound Ti_3Ir at present investigated occupies other interstitial—or at least additional interstitial—sites than in Nb_3Sn where it is located on tetrahedral sites such as those shown in figure 1 [6].

5. Conclusions

We determined the spin-lattice relaxation rate of hydrogen interstitials in the A15 compound Ti_3Ir from pulsed NMR measurements. The measured relaxation rates can quantitatively be explained by superposition of Korringa relaxation and dipolar relaxation due to the diffusion of the hydrogen. The inverse mean residence time τ^{-1} of the hydrogen was determined from the dipolar relaxation rate with the help of a modified BPP model. The results for τ^{-1} exhibit a distinct dependence on the hydrogen concentration. The results were compared with those reported from previous studies of the dynamics of hydrogen in the A15 compounds Ti_3Ir and Nb_3Sn .

References

- [1] Muller J 1980 *Rep. Prog. Phys.* **43** 641
- [2] Schlereth M and Wipf H 1990 *J. Phys.: Condens. Matter* **2** 6929
- [3] Schlereth M and Wipf H 1990 *Scr. Metall. Mater.* **24** 1159
- [4] Ziegler G 1968 *Helv. Phys. Acta* **41** 1267
- [5] Sahn P R 1968 *Phys. Lett.* **26A** 459
- [6] Vieland L J, Wicklund A W and White J G 1975 *Phys. Rev. B* **11** 3311
- [7] Huang S Z, Skoskiewicz T, Chu C W and Smith J L 1980 *Phys. Rev. B* **22** 137
- [8] Shamrai V, Bohmhammel K and Wolf G 1982 *Phys. Status Solidi b* **109** 511
- [9] Rama Rao K V S, Mrowietz M and Weiss A 1982 *Ber. Bunsenges. Phys. Chem.* **86** 1135
- [10] Beisenherz D, Guthardt D and Wipf H 1991 *J. Less-Common Met.* **172-4** 693
- [11] Berry B S, Pritchett W C and Bussière J F 1983 *Scr. Metall.* **17** 327
- [12] Junod A, Flukiger R and Muller J 1976 *J. Phys. Chem. Solids* **37** 27
- [13] Abragam A 1961 *The Principles of Nuclear Magnetism* (Oxford: Clarendon)
- [14] Zamir D and Cotts R M 1964 *Phys. Rev.* **134** A666
- [15] Pedersen B, Krogdahl T and Stokkeland O E 1965 *J. Chem. Phys.* **42** 72
- [16] Zogal O J and Cotts R M 1975 *Phys. Rev. B* **11** 2443
- [17] Fukai Y and Kazama S 1977 *Acta Metall.* **25** 59
- [18] Messer R, Blessing A, Dais S, Höpfel D, Majer G, Schmidt C, Seeger A, Zag W and Lässer R 1986 *Z. Phys. Chem., NF, Suppl.* **2** 61